Pergamon

Available online at www.sciencedirect.com
SCIENCE DIRECT®

Cement and Concrete Research 33 (2003) 1755–1763

CEMENT AND CONCRETE RESEARCH

Influence of the aggregate on the electrical conductivity of Portland cement concretes

Antonio Principigallo[a], Klaas van Breugel[b], Giovanni Levita[a,*]

[a]*Department of Chemical Engineering, Industrial Chemistry and Materials Science, University of Pisa, Via Diotisalvi 2, 56126 Pisa, Italy*

[b]*Concrete Structures Group, Stevin Laboratory, Faculty of Civil Engineering and Geosciences, Delft University of Technology, P.O. Box 5048-2600 GA Delft, The Netherlands*

Received 15 August 2002; accepted 22 April 2003

Abstract

The electrical conductivity and compressive strength of several high-performance Portland concretes with different amounts of crushed aggregate and sand have been measured at early age in isothermal conditions (20 °C). The total aggregate volume fraction varied from 0 (plain paste) to 0.75 and a constant weight ratio (1.2) between crushed aggregate and sand was used. The w/c ratio was 0.37 and microsilica (in slurry form) and a superplasticizer in water solution were used.

The time taken before the electrical conductivity began to drop correlated very well with the induction period. The drop of conductivity was slightly delayed by the aggregate. The analysis of the electrical data, by means of different numerical and analytical models [hard core soft shell model (HCSS), differential effective medium theory (DEMT), Lu–Torquato, Maxwell], allowed an estimate of the properties of the interfacial transition zone (ITZ). In particular, an ITZ thickness of about 9 μm and an ITZ to bulk conductivity ratio of ~2.5 were found. The existence of a percolating pathway through the interfacial regions was found by both electrical measurement and modeling when the aggregate volume fractions exceeded 60%. Finally, a new relationship among electrical conductivity, compressive strength, and aggregate amount was derived.

Keywords: Electrical conductivity; Concrete; Interfacial zone; Modeling; Percolation

1. Introduction

Monitoring the properties of manufactured goods is nowadays an essential requirement in quality control regimes particularly for precast structures [1]. The electrical properties of cement pastes have proved to be rather sensitive to minute changes in the microstructure of cementitious materials. Out of the many different techniques used to study the aging of concrete mixes (e.g., electronic microscopy, X-ray diffraction, or thermogravimetry), the dielectric spectroscopy displays high sensibility, versatility, and possibility to operate remotely. In addition, the knowledge of the electrical parameters is useful for the development of accelerated curing processes, for instance, by electromagnetic heating [2–4].

The strength of a concrete cannot be easily related to the strength of the mortar or of the neat paste. The compressive strength of a paste can be 30% higher then that of a mortar and up to 50% higher than that of an ordinary concrete [5,6]. However, the use of low w/c ratios and silica fume can result in a concrete with a strength exceeding that of the neat paste [7,8]. This can be explained by the existence of week bonds between the aggregate surface and the paste; the region around the aggregate particles thus influences the overall behavior of the composite. The same reasoning can be applied to the transport properties such as the electrical conductivity, diffusivity, and permeability [9–11].

Permeability, in particular, was observed to be higher for the mortar than for the cement paste [12] showing a close relation with the electrical conductivity [13]. The aim of this paper is to prove the capability of electrical methods to monitor microstructure changes in concretes and to give an insight into microscopic features such as the properties of the interfacial transition zone (ITZ). A relationship

* Corresponding author. Tel.: +39-50-511-201; fax: +39-50-511-266.
E-mail address: levita@ing.unipi.it (G. Levita).

0008-8846/$ – see front matter © 2003 Elsevier Ltd. All rights reserved.
doi:10.1016/S0008-8846(03)00166-2

Table 1
Mix compositions

Component	Parts by weight
Cement, CEM I 52.5 R ENCI (Blaine 5300 cm^2/g)	100
Microsilica, slurry Heidelberger Bauchemie GmbH, dry content: 51% (B.E.T. 190,000 cm^2/g)	10.5
Naftalene sulfonate Addiment FM951 NBC Bouwstoffen, dry extract: 40%	0.7
Ligninosulfonate Addiment BV1 NBC Bouwstoffen, dry extract: 36%	0.07
Crushed aggregate (4–16 mm)	0 ÷ 302
Sand (0–4 mm)	0 ÷ 250
Total water	37

between conductivity and macroscopic strength was also derived.

We studied the electrical properties of high-performance concretes with a low water content and of a Portland cement paste densified by the addition of silica fume and superplasticizers. The effect of the superplasticizer on the electrical parameters of cement pastes was already studied [14,15]. In this paper, we focus on the influence of the aggregate and we will show how the electrical parameters can be used to sense the microstructure changes.

2. Materials and methods

2.1. Materials

The cement was an OPC type I 52.5 R produced by ENCI. The aggregate was sand (particle size less than 4 mm) and crushed aggregate (size 4-16 mm). A constant weight ratio between the two components was maintained (1.2) for all formulations. Further ingredients were silica fume (in slurry form), a lignosulfonate-based plasticizer, and a naphthalene–sulfonate-based superplasticizer. The w/c ratio was in all cases 0.37. For the actual composition of mixes, see Table 1.

2.2. Compressive strength and split test

The compressive strength was measured on sealed cubes $150 \times 150 \times 150$ mm^3 (NEN 5968). Cubes were cast in

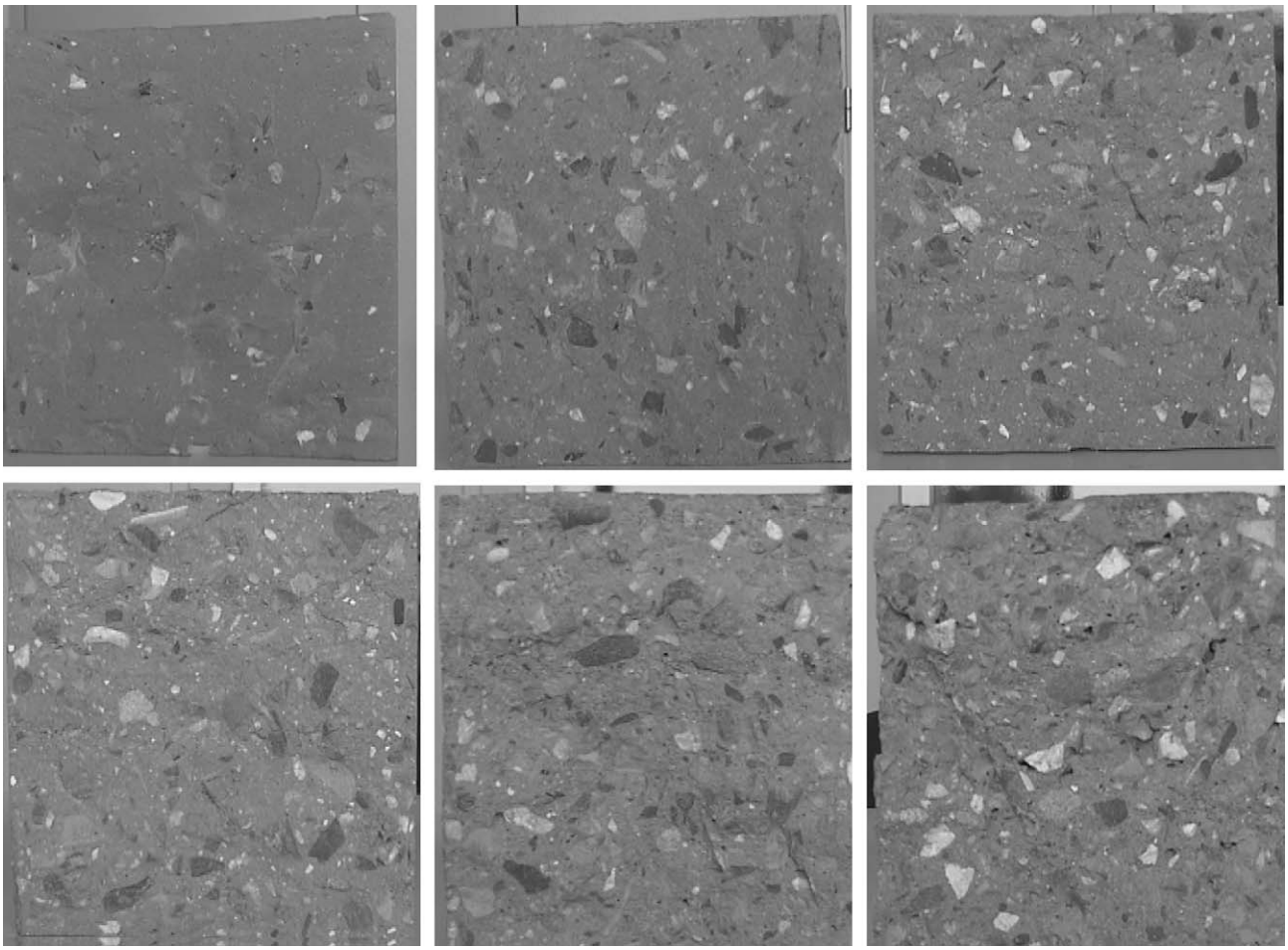

Fig. 1. Fracture surfaces of samples with various aggregate content (split test NEN 5969). Clockwise from top to left: 10%, 30%, 40%, 75%, 60%, and 50%.

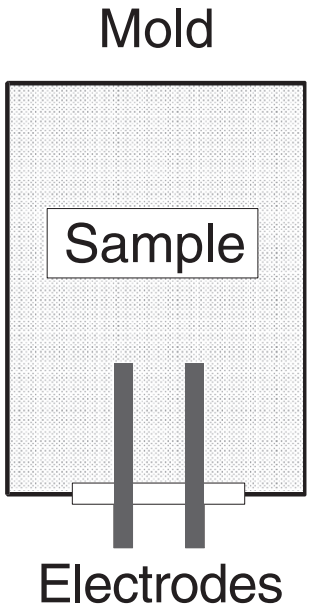

Fig. 2. Experimental setup for the electrical conductivity measurements.

temperature-controlled steel moulds and tested after 8, 24, and 30 h. Some split tests were also performed on cubes after 1-day hydration in order to check the uniformity of the aggregate distribution and absence of bleeding. No aggregate segregation was observed (Fig. 1).

2.3. Electrical conductivity

Electrical conductivity measurements were performed on concrete samples about $150 \times 150 \times 200$ mm^3. The experimental setup is shown in Fig. 2. The temperature was kept at 20 ± 1 °C by means of a cooling system.

The electrical conductivity was measured with the apparatus CONSENSOR [1]. The sensor consisted of two cylindrical rods (10-mm diameter) placed at an axial distance of 30 mm. The device was controlled by a microchip that allowed continuous measuring. Measurements started about 10 min after mixing and were carried out for 5 days. Data were taken at 20 MHz to minimize polarization effects at the electrode/paste interface.

3. Numerical and analytical models

In real concrete, any property within the interfacial region changes gradually through the thickness [16–18]. For the sake of simplicity, we assume such properties to be constant [19] and we treat the ITZ as a real phase. The paste is thus modeled as a two-phase system: the ITZ and the bulk paste, each with different properties [19]. Because of the wall effect, the ITZ contains, at the beginning of hydration, more water [13,18] than the bulk paste.

Several models, i.e., the hard core soft shell model (HCSS) [20], the differential effective medium theory (DEMT) [21,22], and the Lu–Torquato model [19,23], were utilized to study the properties of the ITZ.

3.1. HCSS model

The HCSS, developed at NIST, was utilized to estimate the effect of ITZ on the overall conductivity and to evaluate the percolation properties of the systems. The aggregate was modeled as spherical particles of different radii according to the particle size distribution. The particles were randomly located in the model space (a cube with 30-mm edge).

Aggregate particles (HC) were not allowed to overlap and were surrounded by spherical shells (SS) to represent the ITZ. The interfacial regions were allowed to overlap on one another and also on other aggregate particles. A random walk algorithm was used to estimate the transport properties [23]. A conventional burning algorithm was utilized to check for phase connectivity [20,23].

3.2. DEMT model

The DEMT can be used to estimate the properties of particulate composites [21]. In the dilute limit, assuming that the aggregate volume fraction is small enough so as to neglect interparticle interactions, the following equation applies:

$$\frac{\sigma}{\sigma_b} = 1 - m\phi_{agg} + O(\phi_{agg}^2) \tag{1}$$

where σ and σ_b are the conductivity of the whole system (bulk, ITZ, and aggregate) and of the bulk, respectively; ϕ_{agg} is the aggregate volume fraction and m is a constant that equals $-3/2$ for insulating spherical inclusions of any size distribution embedded in a homogeneous conductive medium (Maxwell equation). In general, the parameter m depends on the conductivity of the interface, σ_{ITZ}, as well as on that of the bulk and of the aggregate, σ_a. It also depends on the mean radius of the solid particles, r, and the ITZ thickness, t_{ITZ}, according to the following equation [22]:

$$m = \frac{3[(\sigma_a - \sigma_{ITZ})(2\sigma_{ITZ} + \sigma_b) + ((r + t_{ITZ})/r)^3(\sigma_a + 2\sigma_{ITZ})(\sigma_{ITZ} - \sigma_b)]}{[(\sigma_{ITZ} + 2\sigma_b)(\sigma_a + 2\sigma_{ITZ}) + 2(r/(r + t_{ITZ}))^3(\sigma_a - \sigma_{ITZ})(\sigma_{ITZ} - \sigma_b)]} \tag{2}$$

For high aggregate content, Eq. (2) fails. The conductivity is then to be found by solving the following equation:

$$\int_{\sigma_b}^{\sigma(\phi_{agg})} \frac{d\sigma_b'}{m(\sigma_b')\sigma_b'} + \ln(1 - \phi_{agg}) = 0. \tag{3}$$

3.3. Lu–Torquato model

The model developed by Lu and Torquato [19,23] allows the calculation of the total volume fraction, V_{ITZ}, of the

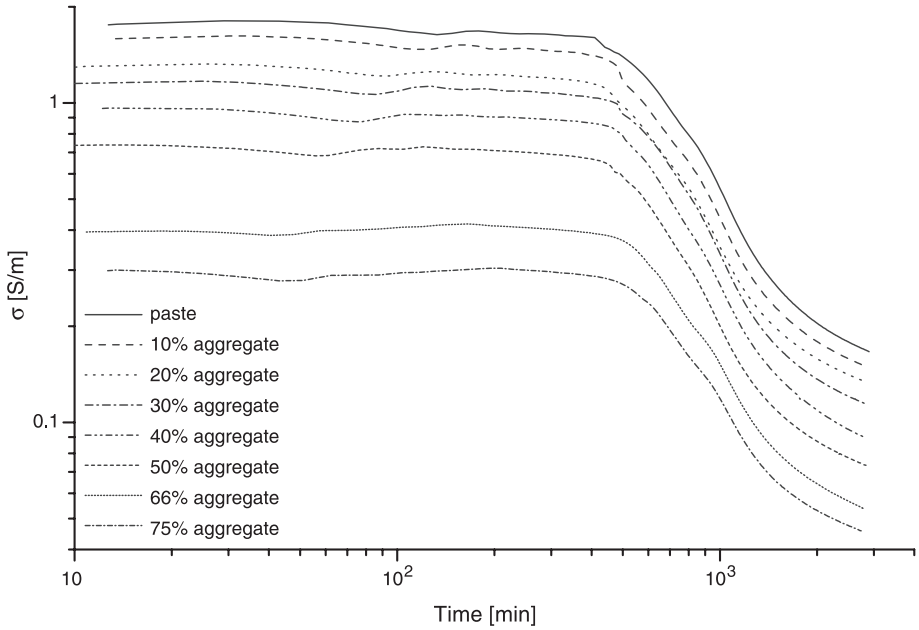

Fig. 3. Electrical conductivity as a function of time for different aggregate contents.

interfacial zone around an assembly of randomly positioned spheres of various sizes:

$$V_{ITZ} = 1 - \phi_{agg} - (1 - \phi_{agg})\exp[(-\pi\rho(ct_{ITZ} + dt_{ITZ}^2 + gt_{ITZ}^3)] \quad (4)$$

where ρ (the number of particles per unit volume), c, d, and g are analytical functions that depend on the aggregate particle size distribution. This complex equation accounts for the overlapping of spherical shells surrounding each particle at high aggregate concentrations.

4. Results and discussion

4.1. Electrical conductivity

For all formulations, the conductivity decreased with time as a consequence of microstructural modifications (changes in the chemical composition of the pore fluid played a minor role). The continuous liquid phase, the main path for the current flow, steadily decreases during the hydration. In the σ-log(time) curves, two transitions were observed, Fig. 3. The first, at early age, is related to the set

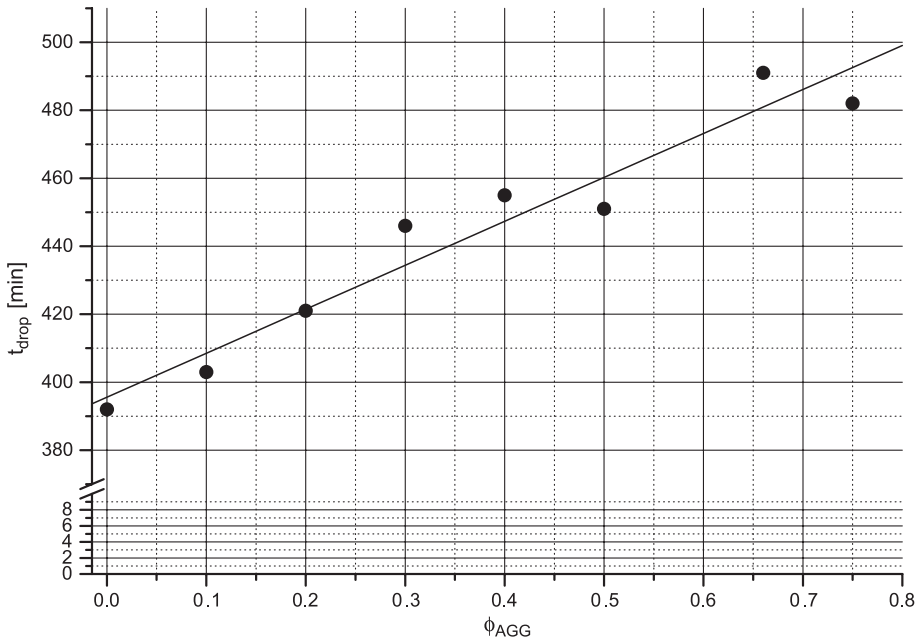

Fig. 4. Time to drop of the electrical conductivity as a function of the aggregate content.

of the paste and the second reflects the depercolation of solution filled porosity [24]. The small increase in conductivity at the very beginning has been attributed to thermal effects [25].

Data in Fig. 3 indicate that the electrical conductivity of concrete regularly decreases on increasing the aggregate content. The early conductivity varied from ~1.8 S/m, for the plain paste, to ~0.3 S/m, for the concrete with 75% aggregate content. These effects were expected because the electrical conductivity of the aggregate is much lower (~0.002 S/m [1]) than that of the paste.

The time evolution of the conductivity of concrete samples was similar to that of the plain paste; this confirms that the electrical behavior of concrete is substantially dominated by the cementitious matrix. However, the drop in conductivity, indicative of the duration of the induction period [15], was progressively delayed as the aggregate content increased. As shown in Fig. 4, the time to drop, t_{drop}, linearly grows with the aggregate content; the time to drop for the 75% aggregate formulation was delayed by about 2 h. Several effects influence the time and composition dependence of conductivity.

1. On decreasing the cement content, the heat of hydration diminishes and temperature variations are less likely to occur. Since we operated in isothermal conditions, this effect should be negligible.
2. Due to the wall effect, the water content is higher in the ITZ than in the bulk. A higher w/c ratio was already seen to delay the set point [26]. Since the conductivity of cement pastes depends on the amount of water, the water depleted bulk will have a reduced conductivity.
3. On the other hand, a water enriched ITZ have a higher conductivity, particularly when the ITZs become connected.

At moment, we are not able to evaluate the relative importance of the last two effects.

4.2. Influence of the ITZ on the electrical properties

The electrical conductivity of dispersions of nonconductive spheres in conductive media can be described by the Maxwell relations (two-phase model) (Fig. 5) [27,28]:

$$\frac{\sigma}{\sigma_b} = 1 - 3/2\phi_{agg}$$

$$or \qquad (5)$$

$$\frac{\sigma}{\sigma_b} = (1 - \phi_{agg})^{3/2}$$

(σ_b being the bulk conductivity). Data in Fig. 5 indicate that the real conductivity was higher than that expected from Eq. (5) even at low aggregate contents (Maxwell relations strictly hold in the dilute region). As already outlined, the ITZ composition differs from that of the bulk. The system should rather be considered as a three-phase system. Apparently, the ITZ contribution to the overall conductivity is rather large, particularly at high aggregate content (ϕ_{agg}>0.6) and high hydration times. Long-range pathways in Portland cement mortars were found by Shane et. al. [13], using Mercury Intrusion Porosimetry [15], and by Winslow et al. [29].

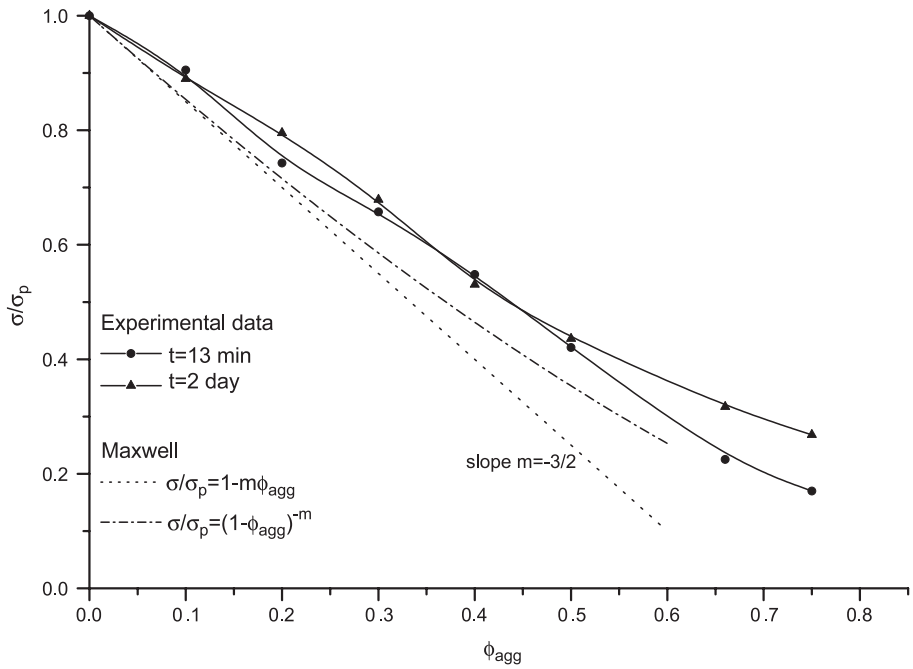

Fig. 5. Normalized conductivity as a function of aggregate content (dotted and dashed lines are the Maxwell equations).

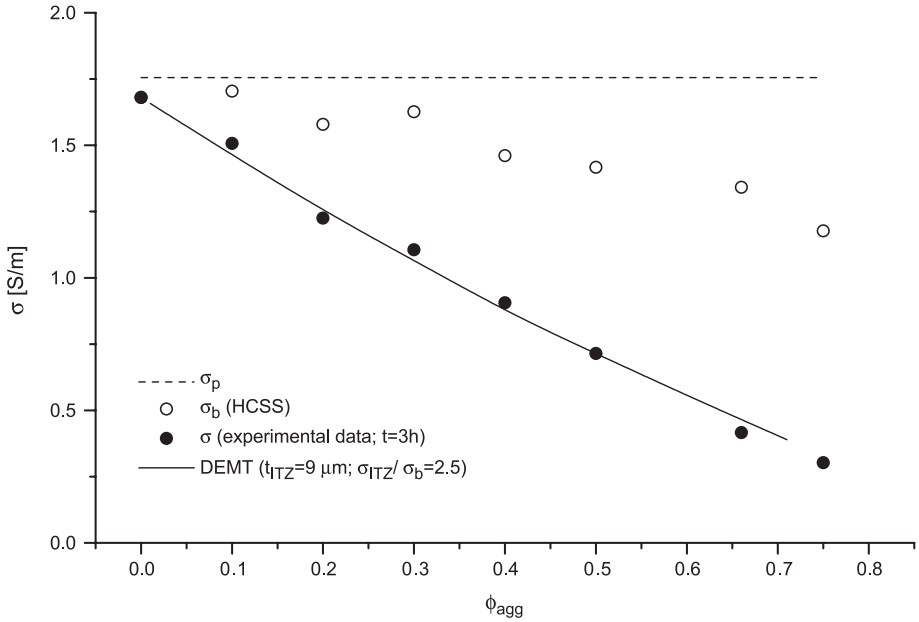

Fig. 6. Electrical conductivity of fresh concrete as a function of aggregate content (the continuous line is from DEMT simulation; the open dots are the bulk paste conductivity from HCSS model; the conductivity of the plain paste is given by the horizontal dashed line).

4.3. Numerical modeling

A combination of HCSS and DEMT models was utilized to investigate the interface properties of the concretes. Input parameters were the thickness of the ITZ and the interface to bulk conductivity ratio, σ_{ITZ}/σ_b. The initial values of these parameters were the mean average size of cement particles (9 μm in our case) and 2.5 according to [15,20,30]. This values, fed to the HCSS model, allowed to evaluate the effect of the aggregate on the conductivity of the bulk paste (see point 2 above). Once the bulk conductivity was known, we calculated the overall conductivity by means of the DEMT model. The good match between model and experimental data, Fig. 6, indicates that the values of thickness and conductivity of the ITZ were correct.

4.4. Percolation of the ITZs

In the diluted region, the ITZs that surround the aggregate particle are far apart. On increasing the particle density, the distance among the ITZs decreases and, eventually, vanishes. If we normalize the conductivity of each sample

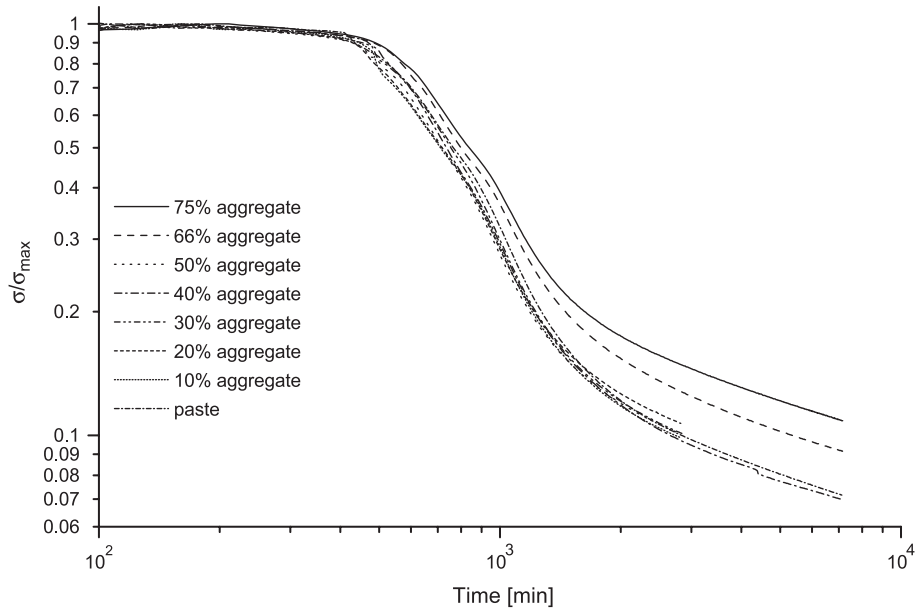

Fig. 7. Normalized electrical conductivity as a function of time for different aggregate contents.

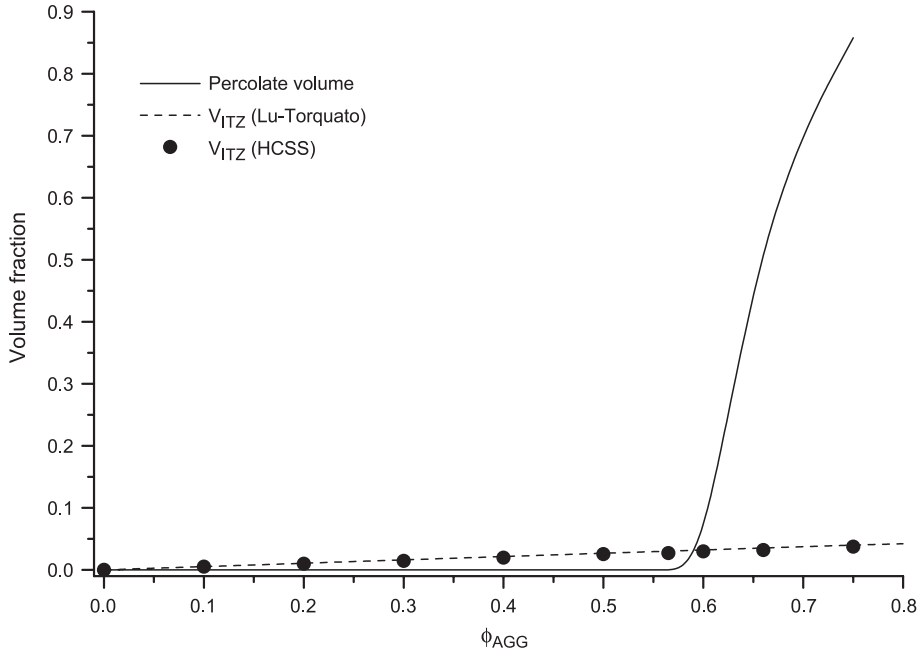

Fig. 8. Volume fraction of the ITZ according to the HCSS and Lu–Torquato models. The percolated volume (aggregate plus ITZ) is also shown.

to the initial value, we see that a single master curve is obtained for formulations with aggregate contents less than ~0.6, Fig. 7. For higher loadings, the conductivity remained higher at long hydration times. This can be easily explained by admitting the formation of a continuous (percolated) high conductivity path from the superposition of ITZs. At high loadings, the flux of charge carriers apparently takes place more and more through the interfacial regions rather than through the bulk CSH.

We computed the total volume of ITZs by both the HCSS and DEMT models, Fig. 8. Due to the reduced thickness of the ITZ, its volume is relatively small. By adding to the volume of each aggregate particle the volume of the relative ITZ, it was possible to evaluate the aggregate content that would allow the percolation of the outer ITZs. Fig. 8 indicates that the solid critical content is about 0.6, which well correlates with the value at which deviations were observed in Fig. 7.

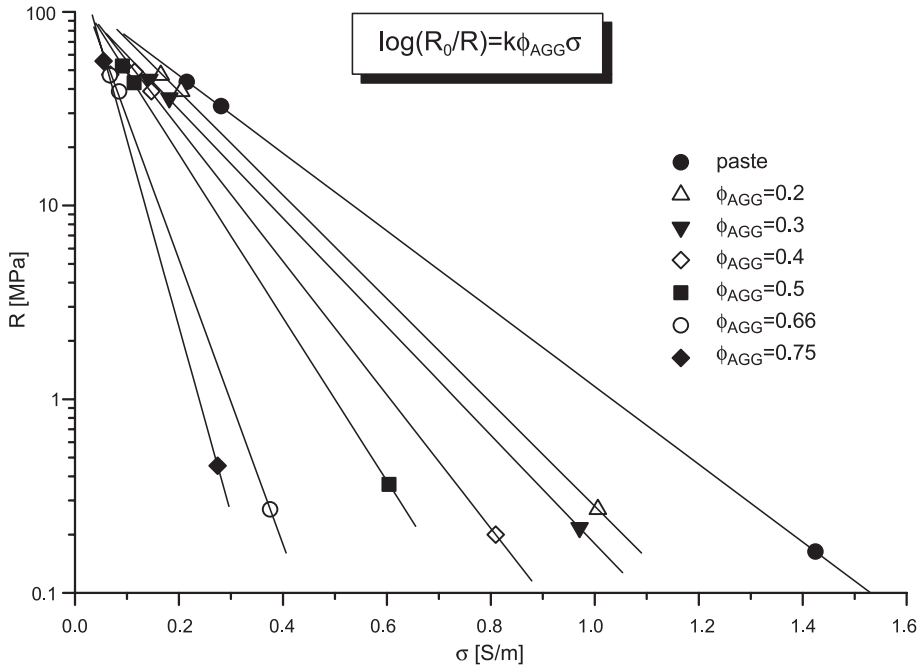

Fig. 9. Strength–conductivity relationship for the mixes. Strength measured at 8, 24, and 30 h.

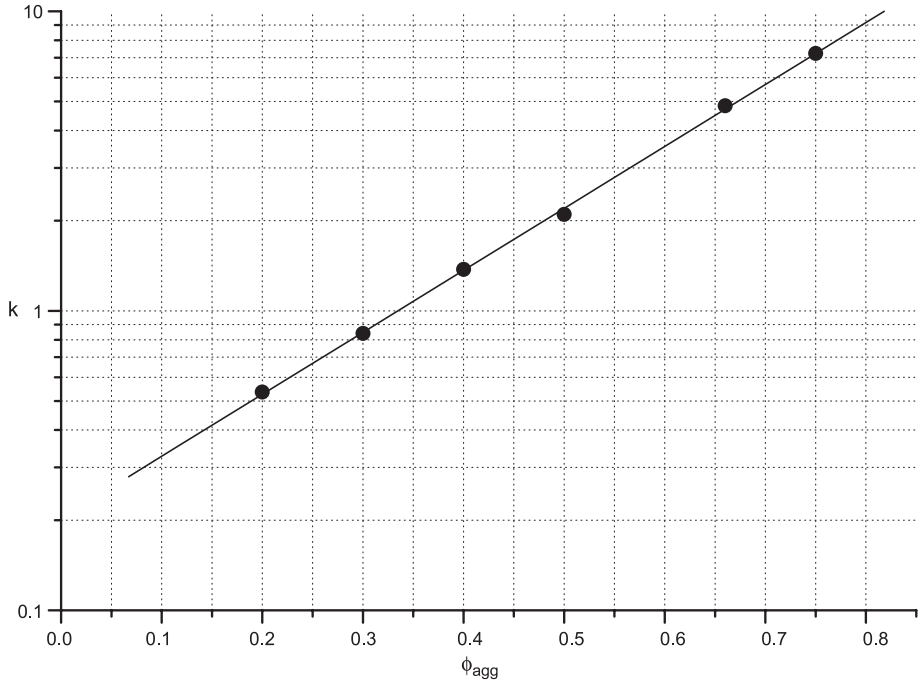

Fig. 10. Dependence of k (Eq. (7)) on the volume fraction of the aggregate.

4.5. Strength–conductivity relationship

A relationship between conductivity and strength has been previously found for concrete [1]. We generalize such relationship to concretes with various aggregate contents. All data in Fig. 9 in which the compressive strength is plotted as a function of electrical conductivity for all formulations obey the following equation:

$$\log\left(\frac{R_0}{R}\right) = k(\phi_{agg})\phi_{agg}\sigma \tag{6}$$

where R is the compressive cube strength (MPa), R_0 and k are constants for each formulation. R_0 can be considered as an intrinsic property of a specific mix; values vary from 118 to 200 MPa with increasing the aggregate volume fraction.

Also the parameter k depends on the aggregate content. The linear plot in Fig. 10 indicates that a power law relationship holds between $k(\phi_{agg})$ and composition:

$$k(\phi_{agg}) = 10^{(a\phi_{agg}-b)} \tag{7}$$

The parameters $a = 2.07 \pm 0.02$ and $b = 0.69 \pm 0.01$, on the contrary, are constant and mix independent.

5. Conclusions

The electrical conductivity and compressive strength of several Portland cement concretes (total aggregate content 0–75%) have been measured at early ages in isothermal conditions at 20 °C. The electrical conductivity was affected by both hydration and aggregate content. A delaying effect ($\sim$2 h) of the aggregate on the first inflection point of the conductograms (related to setting) was clearly observed.

The extent and properties of the interfacial zones were studied by analyzing the electrical conductivity of all formulations by means of several numerical models (HCSS, DEMT, Lu–Torquato, Maxwell). It has been found that even the properties of the bulk cement paste are affected by the presence of the solid aggregate particles, most likely for a redistribution of porosity. The study has clearly shown that the interfacial region, whose porosity and electrical conductivity exceed those of the bulk paste, percolate at high solid contents. A percolating pathway appeared for aggregate volume fractions higher than 60%. Finally, a relationship among electrical conductivity, compressive strength, and aggregate concentration was found.

The sensitivity and speed, along with the possibility to perform remote measurements, confirm the electrical methods as a viable technique to monitor the properties of high-performance concretes.

Acknowledgements

The assistance of Mr. E. Horeweg and Mr. R. Mulder in performing the experiments is gratefully acknowledged.

References

[1] A. van Beek, Dielectric properties of young concrete-non-destructive dielectric sensor for monitoring the strength development of young concrete, PhD Thesis, Delft University of Technology, Delft, 2000.

[2] M. Leivo, Radio wave heating of concrete, Cem. Concr. Res. 26 (5) (1996) 677–682.
[3] G. Gallone, G. Levita, A. Marchetti, F. Baldi, A. Principallo, G. Guerrini, Maturazione a microonde di materiali cementizi a elevate prestazioni, AIMAT Congress, Spoleto, Italy, vol. 1, 2000 July, p. 135.
[4] G. Levita, A. Principallo, G. Gallone, A. Marchetti, G.L. Guerrini, Metodi elettrici nella tecnologia di malte e calcestruzzi, 13th CTE Congress, Pisa, vol. I, 2000 November, p. 287.
[5] K.M. Alexander, J.H. Taplin, J. Wardlaw, 5th International Symposium of Cement Chemistry, Correlation of Strength and Hydration with Composition of Portland Cement, Tokyo, vol. III, 1968, pp. 152–166.
[6] H.J. Gilkey, Water-cement ratio versus strength: another look, ACI J. 57–55 (1961) 1287–1311.
[7] K. Walz, Beziehung zwischen wasserzementwert, normfestigkeit des zements (DIN 1164) und betondruckfestigkeit, Beton 11 (1970) 499–503.
[8] K.L. Scrivener, A. Bentur, P.L. Pratt, Quantitative characterization of the transition zone in high strength concretes, Adv. Cem. Res. I (4) (1988) 230–237.
[9] X. Ping, J.J. Beaudoin, R. Brousseau, Flat-aggregate Portland cement paste interfaces: I. Electrical conductivity models, Cem. Concr. Res. 21 (1991) 515–522.
[10] U. Costa, M. Facoetti, F. Masazza, Permeability of the cement-aggregate interface: influence of the type of cement, water/cement ratio and superplasticizer, in: E. Vazquez (Ed.), Admixtures for Concrete: Improvement of Properties, Chapman & Hall, London, 1990, pp. 392–401.
[11] K.L. Scrivener, K.M. Nemati, The percolation of pore space in the cement paste/aggregate interfacial zone of concrete, Cem. Concr. Res. 26 (1) (1996) 35–40.
[12] P. Halamicova, R.J. Detwiler, D.P. Benz, E.J. Garboczi, Water permeability and chloride ion diffusion in Portland cement mortars: relationship to sand content and critical pore diameter, Cem. Concr. Res. 25 (4) (1995) 790–802.
[13] J.D. Shane, T.O. Mason, H.M. Jennings, E.J. Garboczi, D.P. Denz, Effect of the interfacial transition zone on the conductivity of Portland cement mortars, J. Am. Ceram. Soc. 83 (2000) 1137–1144.
[14] G. Levita, A. Marchetti, G. Gallone, A. Principallo, G.L. Guerrini, Electrical properties of fluidified Portland cement mixes in the early stage of hydration, Cem. Concr. Res. 30 (2000) 923–930.
[15] J.M. Torrents, J. Roncero, R. Gettu, Utilization of impedance spectroscopy for studying the retarding effect of a superplasticizer on the setting of cement, Cem. Concr. Res. 28 (9) (1998) 1325–1333.
[16] K. van Breugel, Simulation of hydration and formation of structure in hardening cement-based materials, PhD Thesis (revised edition), Technical University Delft, 1997.
[17] E.A.B. Koenders, Simulation of volume changes in hardening cement-based materials, PhD Thesis, Technical University Delft, 1997.
[18] D.B. Benz, E.J. Garboczi, P.E. Stuzman, Computer modelling of the interfacial transition zone in concrete, in: J.C. Maso (Ed.), Interfaces in Cementitious Composites, E & FN Spon, London, 1993, pp. 259–268.
[19] E.J. Garboczi, D.P. Bentz, Multi-scale analytical/numerical theory of the diffusivity of concrete, Adv. Cem. Based Mater. 8 (1998) 77–88.
[20] D.P. Benz, E.J. Garboczi, K.A. Snyder, A hard core/soft shell microstructural model for studying percolation and transport in three-dimensional composite media, NIST. NISTIR, vol. 6265, 1999 January.
[21] R. McLaughlin, A study of the differential scheme for composite materials, Int. J. Eng. Sci. 15 (1977) 237–244.
[22] L.M. Schwartz, E.J. Garboczi, D.P. Bentz, Interfacial transport in porous media: application to D.C. electrical conductivity of mortars, J. Appl. Phys. 78 (1995) 5898–5908.
[23] B. Lu, S. Torquato, Nearest-surface distribution functions for polydispersed particle systems, Phys. Rev., A 45 (8) (1992) 5530–5544.
[24] A. Principallo, G. Levita, A. Marchetti, G. Gallone, G.L. Guerrini, Advancements in modelling the development of microstructure in cement pastes, 7th European Conference on Advanced Materials and Processes, AIM, Rimini, Italy, 2001 June.
[25] A. Principallo, Doctorate dissertation, Politechnic of Milan, Milano, 2002.
[26] J.F. Clemmens, E.J. Sellevold, Correlating the deviation point between external and total chemical shrinkage with setting time and other characteristics of hydrating cement paste, Proceedings of the International RILEM Workshop on Shrinkage of Concrete-Shrinkage 2000, Paris, 2000 October, part I, no. 4.
[27] R. Turner, The electrical conductance of liquid-fluidized beds of spheres, Chem. Eng. Sci. 31 (1976) 487–492.
[28] L. Sigrist, O. Dossenbach, N. Ibl, On the conductivity and void fraction of gas dispersions in electrolyte solutions, J. Appl. Electrochem. 10 (1980) 223–228.
[29] Winslow, M.D. Choen, D.P. Benz, K.A. Snyder, E.J. Garboczi, Percolation and pore structure inmortars and concrete, Cem. Concr. Res. 24 (1994) 25–37.
[30] D.P. Bentz, R.J. Detwiler, E.J. Garboczi, P. Halamicova, L.M. Schwartz, Multi-scale modeling of the diffusivity of mortar and concrete, in: L.O. Nilsson, J.P. Olliver (Eds.), Proceedings of Chloride Penetrations into Concrete, RILEM, 1997.